Mobile Smart Grids: Exploiting the TV White Space in Urban Scenarios

ANGELA SARA CACCIAPUOTI[1,2], (Senior Member, IEEE),
MARCELLO CALEFFI[1,2], (Senior Member, IEEE), FRANCESCO MARINO[1],
AND LUIGI PAURA[1,2], (Member, IEEE)

[1]Department of Electrical Engineering and Information Technologies, University of Naples Federico II, 80125 Naples, Italy
[2]CeRICT, 80125 Naples, Italy

Corresponding author: A. S. Cacciapuoti (angelasara.cacciapuoti@unina.it)

ABSTRACT Due to its attractive characteristics, the TV white space (TVWS) spectrum is considered the ideal candidate to enable the deployment of smart grid networks (SGNs) via cognitive radio paradigm. However, the intermittent availability of the TVWS spectrum as well as its scarcity in urban scenarios could compromise the tight smart grid requirements in terms of reliability, latency, and data rate. This degradation could be even more severe when mobile grid nodes, e.g., electric vehicles, are considered. Stemming from this, we first develop an analytical framework to account for the mobility in SG scenarios. Then, we design a switching procedure based on the use of two different bands: TVWS spectrum and Industrial, Scientific and Medical (ISM) spectrum. The switching procedure selects, among the available spectrum bands, the one maximizing the achievable throughput at an arbitrary SGN. Such a procedure accounts for the presence of interfering SGNs on the TVWS spectrum through both their traffic and mobility patterns. By wisely using both the ISM and the TVWS spectrum, the proposed switching procedure is able to: 1) increase the achievable data rate, and to 2) reduce the outage event rate, improving the reliability and the latency of the smart grid communications. Moreover, we show the performance of the proposed switching procedure depends largely on the time devoted to sense. Hence, the proper setting of such a parameter is critical for the performance of any SGN. For this, we derive an optimization criterion maximizing the throughput under the constraint of bounding the outage rate. The theoretical analysis is validated through extensive numerical simulations.

INDEX TERMS Smart grid, cognitive radio; channel outage, TV white space.

I. INTRODUCTION

The TV White Space (TVWS) spectrum has been recently recognized by the research community as the ideal candidate to accommodate the rapidly increasing demand for wireless broadband communications in Smart Grid Networks (SGNs) via Cognitive Radio (CR) paradigm [1]–[7]. In fact, traditionally SGNs operate in the ISM bands. This implies that traffic congestion and interference can significantly degrade the SGNs communication performance, since sharing the spectrum with other wireless systems is unavoidable. Therefore, by deploying SGNs jointly operating in TVWS and ISM bands, additional spectrum resources can be made available to the SGNs needs, thus reducing the degrading-impact of congestion and interference. Additionally, the excellent TVWS propagation conditions result also in a lower

sensitivity to obstacles when compared to spectrum bands in the gigahertz order. Furthermore, differently from other CR-based technologies and in agreement with the current regulations [8]–[10], the TVWS paradigm simplifies the license-exempt (secondary) access through the utilization of a geolocation database for incumbent protection [8]–[12].

For an effective deployment of TVWS-enabled SG networks, some crucial challenges must be addressed as described in the following. Experimental studies have shown that the number of TVWS channels is significantly limited in urban areas [13], [14]. Hence, it is likely that multiple closely-located, heterogeneous and independently-operated SGNs are authorized to use the same TVWS channel, as depicted in Figure 1. Since so far there are no regulatory requirements for the coexistence among heterogeneous

FIGURE 1. TVWS Smart Grid Scenario: SGNs coexisting within the same geographical area could interfere.

networks over TVWS [12], [15], their transmissions may collide, leading so to a performance degradation and to an inefficient use of the TVWS spectrum. This degradation could be even more severe in environments characterized by mobile grid nodes such as on-line Electric Vehicles (EVs) [16]–[19], since the mobility changes the network topology [20], [21].

Stemming from the above considerations, it is clear that a SGN cannot rely only on the TVWS spectrum for its communication needs. In fact, the intermittent availability of such a spectrum, due to either the presence of incumbents or the presence of other interfering SGNs, could compromise the tight SG requirements in terms of reliability, low temporal latency and high data-rates.

For this, in this paper, we propose an optimal switching procedure aiming at maximizing the achievable throughput at an arbitrary SGN, by accounting for the presence of interfering SGNs on the TVWS channels through both their traffic and mobility patterns.

Specifically, we first develop an analytical framework to account for the mobility in SG scenarios. Then, we propose a switching procedure based on the use of two different bands: TVWS spectrum and ISM spectrum. This switching procedure, as detailed in Section III, relies on the capability of the arbitrary SGN to sense the available TVWS spectrum for discovering the interference generated by any closely-located SGN. By wisely using both the ISM and the TVWS spectrum, the proposed switching procedure significantly improves the SG performance in terms of reliability as well as temporal latency and data-rate, since it jointly overcomes: i) the intermittent availability of the TVWS spectrum due to either the incumbent protection or the presence of interference; ii) the high outage rate of the ISM band.

Through the paper, we show the performance of the proposed switching procedure is controlled by the duration of the time devoted to sense the TVWS spectrum, namely, the sensing time. More in detail, we prove there exists a trade-off: i) the shorter is the sensing time, the longer is the portion of time devoted to packet transmission and hence the larger is the achievable throughput; ii) the longer is the

sensing time, the lower is the outage event rate. Hence, the proper setting of the sensing time is critical for the performance of the proposed procedure. This is even more critical in the considered Smart Grid scenarios, characterized by high communication demands associated with the need of reliable communications. For this, through the paper, we derive an optimization criterion for the switching procedure able to maximize the throughput for a given outage rate constraint. Furthermore, for the optimization problem we provide a closed-form expression of the minimum sensing time satisfying the constraint on the outage rate. Finally, we validate the theoretical analysis through extensive numerical simulations.

The rest of the paper is organized as follows. In Section II, we discuss the relevant literature. In Section III, we describe the network model along with some preliminaries. In Section IV, we design the analytical framework and we derive the optimization criterion. In Section V, we validate the theoretical analysis with a user case. In Section VI, we conclude the paper and, finally, some proofs are gathered in the Appendix.

II. RELATED WORKS
Very recently, the adoption of the Cognitive Radio (CR) paradigm for designing Smart Grid communications has gained great attention. In [22], the authors analyze the impact of the channel outage on the Demand/Response Management (DRM) control performance, by proposing a cognitive-based two-way communication switching procedure to reduce the channel outage. In [1], the authors consider the application of the CR paradigm in the Smart Grid scenario, in order to provide a more reliable and stable communication with the DRM. They propose to exploit, beside the traditional temporal spectrum opportunities, the spatial spectrum opportunities as well. In [23], the authors carry out a study on a two-way cognitive-based switching procedure, by evaluating the sensing-time maximizing the transmission opportunities under a sensing accuracy constraint. In [4], the TVWS spectrum is utilized to maximize the achievable data rate but neither the mobility effects or the availability of multiple TVWS channels are considered. Unlike all the cited papers, in this work not only the peculiar and unique properties of the TVWS are taken into account but the analysis is carried out considering the impact of mobility within the Smart Grid paradigm. To the best of our knowledge, this is the first work that accounts for the mobility effects in the smart grid scenarios.

Indeed, mobility is a tight and urgent topic that needs to be addressed in SG scenarios, as widely-recognized by the literature [16]–[19]. In fact, nowadays Electric Vehicles (EVs) are considered key SG entities, due to the numerous services offered to the SG by the bidirectional energy exchange between EVs and power grid [24], [25]. Furthermore, the depletion of petroleum and the global warming make the EVs the most promising means of transport. According to a recent forecast [19], the EV penetration level will reach

35 percent, 51 percent, and 62 percent by 2020, 2030, and 2050, respectively. Moreover, in [17], real-world successful deployments at various public sites of online EVs, based on a inductive power transfer system, have been described. Stemming from above, it is clear that the widespread adoption of EVs and more in general of mobile grid nodes brings new challenges to the operation of the smart grid, since the mobility changes the network topology.

III. NETWORK MODEL AND PRELIMINARIES

In this section, we first describe the system model in Sec. III-A. Then, in Sec. III-B, we collect several definitions that will be used through the paper.
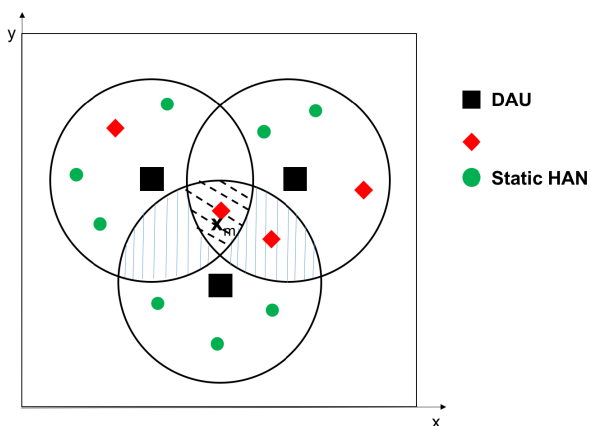

FIGURE 2. Example: *m*-th mobile HAN covered by three different NANs.

A. NETWORK MODEL

We consider the Smart Grid scenario depicted in Figures 1-2. Specifically, a Home Area Network (HAN) is composed by a HAN Gateway (HG) serving multiple smart meters, and it can be either a static HAN (s-HAN, e.g., a building) or a mobile HAN (m-HAN, e.g., a vehicle). The HG is responsible for reporting the meter data periodically collected within its HAN to the Data Aggregate Unit (DAU) as well as to deliver data received by the DAU towards the smart meters. Multiple HGs connected to the same DAU constitute a Neighborhood Area Network (NAN).

Each HG is equipped[1] with a single radio interface operating either: i) within an ISM channel, freely; ii) within a TVWS channel, once authorized by its DAU. Differently, each DAU is equipped with multiple network interfaces and it is responsible for choosing (selecting) the TVWS channel to be used for the HANs communications, among the available ones. Specifically, each DAU selects the best channel by contemporaneously sensing the NAN interference on the available channels through its multiple interfaces. Since experimental studies have shown that the number of TVWS

channels is significantly scarce in urban areas [13], the number of required interfaces is very small, in the order of 2 or 3 elements. Therefore, the assumption is not restrictive in terms of complexity.

1) PROPOSED SWITCHING PROCEDURE

As mentioned in Section I, each DAU obtains the list of TVWS channels free from incumbents by accessing to a geolocation database, referred to as White Space DataBase (WSDB), as required by the current regulations and standards [8], [9], [27], [28]. Experimental studies have shown that the number of TVWS channels is significantly scarce in urban areas [13]. Accordingly, it is likely that the multiple closely-located DAUs receive from the WSDB the same list constituted by few available TVWS channels. Hence, in absence of coordination, any DAU aiming at maximizing the data rate achievable within its NAN must assess the presence of interfering NANs by sensing the TVWS channel for a certain amount of time, say τ. If the sensing declares the TVWS channel free from interference, the DAU authorizes, through a control packet sent on the ISM channel, its HANs to communicate over such a TVWS channel for the remaining time $T - \tau$. Otherwise, the DAU instructs the HANs, again through a control packet sent on the ISM channel, to continue to use the ISM channel.

Stemming from the above description, it is clear that the network operates in a time-slotted fashion[2] of duration T, as described in the following:

- The portion τ of T is devoted by the DAU to sense the TVWS channels declared free from incumbents by the WSDB;
- During τ, the HANs of the considered NAN communicate through ISM band;
- After τ, the HANs receive though the ISM band the DAU control packet to be instructed about which channel they should use. This process is very fast, and let say it requires a time λ;
- In the remaining part of time T, i.e., $T - \tau - \lambda$, the HANs use either the TVWS channel or the ISM channel, accordingly to the DAU sensing process result.

2) ORDERED CHANNEL LIST

In the following we denote with $\mathcal{C} = \{c_1, \ldots, c_B\}$ the list of TVWS channels free from incumbents as it results by querying the WSDB, ordered according to the expected channel throughput $\mathcal{T}_{c_i}$, i.e., $\mathcal{T}_{c_i} \geq \mathcal{T}_{c_{i+1}}$ for any $i \in \{1, \ldots, B-1\}$. In fact, although different metrics can be chosen to order the channels (e.g., channel capacity, delay), very recently [29] it has been proved that the throughput order maximizes the overall throughput achievable by an arbitrary TVWS device. The channel order represents the priorities for the TVWS channel utilization. Specifically, the DAU instructs its HANs to use the TVWS channel c_i if and only if: a) all the TVWS

---

[1]Such an assumption is reasonable since low cost is a strong requirement for the gateways, whereas it is reasonable to assume a DAU equipped with multiple network interfaces [26].

[2]We underline that we do not assume any form of synchronization among the NANs, due to the lack of any kind of cooperation. Hence each NAN is characterized by its own T and τ.

TABLE 1. Performance evaluation parameter setting.

Symbol	Definition	Fig. 4	Fig. 5	Fig. 6	Fig. 7-8
N	number of NANs		5		
$\lvert S_n \rvert$	number of s-HANs belonging to the n-th NAN		$2 \; \forall \, n$		
M	number of m-HANs		6		
$f_{\mathbf{X}_m}(\mathbf{x}_m)$	PDF of the m-th mobile HAN steady-state spatial dist.		generated according to the Random Walk model		
B	number of TVWS channels	3	3	1-3	3
$R^{\text{int}}_{\omega,\omega_\ell}/a$	normalized interference range		$28/75 \; \forall \, n, \ell$		
R_n/a	normalized transmission range		$R^{\text{int}}_{\omega,\omega_\ell}/2 \; \forall \, n$		
W	channel bandwidth		6MHz		
$\mathcal{T}^{\text{ISM}}$	expected throughput on the ISM channel		11Mbps	$\{1,2,5.5,11\}$Mbps	
$\mathcal{T}_c$	expected throughput on c-th TVWS channel		26.7Mbps $\forall \, c$	$\{12,16,18,20,24,26.7\}$Mbps	
$P^{\text{ISM}}_{\text{out}}$	outage probability on the ISM channel		0.3		
P^c_{out}	outage probability on the c-th TVWS channel		$0.03 \; \forall \, c$		
λ	control packet transmission time		$54\mu s$		
$P^{\text{min}}_{\text{sw}}$	switching probability constraint		0.1		
T	time-slot duration		1 s		
τ	interference-sensing time		10ns - 100ms		
γ_c	SNR on the c-th TVWS channel	-20dB	$\{-10,-15,-20\}$dB	-20dB	-10dB

channels with higher priority $c_1, \ldots, c_{i-1}$ have been declared unavailable due to neighbor NAN activities by the sensing procedure; b) the TVWS channel c_i has been declared available by the sensing procedure. In a nutshell, we guarantee that the selected channel is the one, among the channels free from neighbor NAN interference, that maximizes the expected throughput.

B. PRELIMINARIES

In the following, we introduce some assumptions and definitions adopted through the paper. The utilized symbols are synthesized in Table. 1.

We assume that N NANs are geographically co-located within a network region $\mathcal{A}$, assumed[3] either a line or a square to simplify the region representation within the figures. As mentioned in Sec. III-A, each NAN is served by a DAU, hence there exists a one-to-one mapping between NANs and DAUs. In the following, we denote with $\Omega = \{\omega_1, \ldots, \omega_N\}$ the set of NANs or, equivalently, the set of DAUs. Furthermore, we assume that the HANs belonging to a certain NAN can be static as well as mobile.

Each static HAN belongs to a unique NAN, and clearly the mapping doesn't change over time. In the following, we denote with $\mathcal{S}_n = \{h_1, \ldots, h_{S_n}\}$ the set of static HANs of the n-th NAN, whose cardinality is $\lvert \mathcal{S}_n \rvert = S_n$. The overall number S of static HANs deployed within the entire network region $\mathcal{A}$ is $S = \sum_{\omega_n \in \Omega} \lvert \mathcal{S}_n \rvert = \sum_{\omega_n \in \Omega} S_n$.

Differently, each mobile HAN moves within the network region according to an arbitrary mobility model[4] and, hence, it establishes connections with different NANs as time passes. We denote with $\mathcal{M} = \{m_1, \ldots, m_M\}$ the set of mobile HANs roaming within the network region $\mathcal{A}$, and with $f_{\mathbf{X}_m}(\mathbf{x}_m)$ the

[3]This assumption is not restrictive since equation (4) holds for any mono- or bi-dimensional regions.

[4]The analysis carried out within the manuscript does not rely on the specific adopted mobility model. In fact, equation (4) is given in a general formulation, through the pdf $f_{\mathbf{X}_m}(\mathbf{x}_m)$ of the steady-state spatial distribution characterizing the arbitrary mobility model. In Sec. V, for the sake of presentation, we choose as mobility model the widely-adopted Random Walk.

probability density function (pdf) of the steady-state spatial distribution of the m-th mobile HAN.

Definition 1: Let $\mathbf{x}_m(t) \in \mathbf{A}$ denote the position of the arbitrary m-th mobile HAN at time t and let $\mathbf{x}_n \in \mathbf{A}$ denote the position of the arbitrary n-th DAU. The m-th mobile HAN may connect to the n-th DAU at time t when their relative distance is smaller than the DAU *transmission range R_n*:

$$\lVert \mathbf{x}_m(t) - \mathbf{x}_n \rVert \leq R_n \tag{1}$$

The probability of this event is referred to as *connection probability* and it is denoted as ψ_n^m. Such a probability is evaluated in Section IV-A.

In the following, we focus our attention on the arbitrary n-th NAN, say ω. Hence, for the sake of notation simplicity, we omit the n-dependence where applicable, i.e., $\mathbf{x} \stackrel{\triangle}{=} \mathbf{x}_n$.

Definition 2 (Interfering NAN): Let $\mathbf{x}_\ell \in \mathbf{A}$ denotes the position of the ℓ-th DAU. The necessary condition so that the ℓ-th NAN transmissions over a certain TVWS channel, say c, interfere the communications of the arbitrary NAN ω over the same TVWS channel c during the arbitrary time slot k, is that the mutual distance between the two DAUs is smaller than their *interference range $R^{\text{int}}_{\omega,\omega_\ell}$*, i.e.:

$$\lVert \mathbf{x}_\ell - \mathbf{x} \rVert \leq R^{\text{int}}_{\omega,\omega_\ell} \tag{2}$$

Remark 1 The interference range $R^{\text{int}}_{\omega,\omega_\ell}$ depends mainly on the DAU transmission ranges over the considered TVWS channel, their receiving sensitivity, and the adopted channel model [30]. Hence, the widely-adopted geometric model [15], [30], used in Def. 2, allows us to account for the aforementioned system/environmental parameters. Moreover, we note that the condition in Def. 2 is a necessary condition for having interference, since, when $\lVert \mathbf{x}_\ell - \mathbf{x} \rVert > R^{\text{int}}_{\omega,\omega_\ell}$, no active HAN belonging to ω_ℓ falls within the communication range of any HAN belonging to ω.

We denote with Λ_ω the *interfering set* of NAN ω, i.e., the set of NANs that may interfere with NAN ω communications over the TVWS channel c. We note that we do not stress the dependence of Λ_ω from c, since as mentioned before,

the multiple closely-located DAUs belonging to Λ_ω likely receive from the WSDB the same list $\mathcal{C} = \{c_1, \ldots, c_B\}$ of TVWS channels free from incumbents. Hence, the interfering set of NAN ω is the same for each $c \in \mathcal{C}$.

Definition 3 (Activity Probability): P_ℓ^c denotes the probability of the ℓ-th NAN $\in \Lambda_\omega$ using the TVWS channel c in the arbitrary time slot k.

Definition 4 (Overall Activity Probability): P_O^c denotes the overall activity probability on the TVWS channel c, i.e., the probability of at least one NAN belonging to Λ_ω using the TVWS channel c in the arbitrary time slot k.

Definition 5 (Coexistence Detection Probability): The *coexistence detection probability* $P_d^c(\epsilon, \tau)$ denotes the probability of DAU ω declaring the sensed TVWS channel c as unavailable, when channel c is indeed occupied by the communications of at least one NAN in Λ_ω.

In the definition of $P_d^c(\epsilon, \tau)$, we stress its dependence from the decision threshold ϵ, which in turns [31] depends both on the selected sensing technique and the duration τ of the sensing process. In fact, the lower is the sensing time, the lower is the detection probability and hence the higher is the interference caused by the closely-located NANs transmitting on the same TVWS channel on the NAN ω communications.

Definition 6 (Coexistence False-Alarm Probability): The *coexistence false-alarm probability* $P_f^c(\epsilon, \tau)$ denotes the probability of the arbitrary DAU ω declaring the sensed TVWS channel c as unavailable, when channel c is indeed free by the communications of any NAN in Λ_ω. As well-known, the higher is the false-alarm probability $P_f^c(\epsilon, \tau)$, the higher is the amount of TVWS communication opportunities lost.

Definition 7 (Channel Outage Probability): The *channel outage probability* is the probability of a channel being in the outage state, i.e., being unavailable due to adverse wireless propagation conditions. In the following, we denote with $P_{\text{out}}^{\text{ISM}}$ and $P_{\text{out}}^{c_i}$ the outage probability for the ISM channel and the TVWS channel c_i, respectively. In the following, we assume

$$P_{\text{out}}^{\text{ISM}} > \max_{i \in \{1, \ldots, B\}} \{P_{\text{out}}^{c_i}\} \qquad (3)$$

This assumption is justified by accounting for the excellent propagation characteristics of the TVWS spectrum with respect to the ISM spectrum traditionally used in wireless communications.

IV. ANALYTICAL FRAMEWORK
In this section, we first characterize in Sec. IV-A the NAN activity patterns for an arbitrary HAN mobility model, by deriving in Theorem 1 the closed-form expression of the overall activity probability. Then, in Sec. IV-B, stemming from these results, we evaluate with Theorem 2 the overall expected throughput achievable by adopting the proposed switching procedure by the arbitrary *n*-th NAN. Finally, in Sec. IV-C, we derive in Theorem 3 the value of the sensing time that maximize the achievable NAN throughput under reasonable constraints.

A. MOBILITY EFFECTS
Here, we derive the closed form expression of the *overall activity probability* P_O^c on the TVWS channel c through Theorem 1. As a preliminary result, we need first to derive in Lemma 1 the expression of the *mobility-aware activity probability* P_ℓ^c of ℓ-th NAN on the TVWS channel c, which in turn depends on the expression of the *connection probability* ψ_ℓ^m of the m-th mobile HAN being connected to the ℓ-th DAU given in (4).

According to Def. 1, the probability ψ_ℓ^m of the event reported in (1), referred to as *connection probability*, denotes the probability of the m-th mobile HAN being connected to the ℓ-th DAU. This probability can be evaluate as:

$$\psi_\ell^m = \iint_{\mathcal{A}} f_{\mathbf{X}_m}(\mathbf{x}_m) \xi_\ell^m(\mathbf{x}_m) d\mathbf{x}_m \qquad (4)$$

where $f_{\mathbf{X}_m}(\mathbf{x}_m)$ denotes the pdf of the steady-state spatial distribution of the m-th mobile HAN, and $\xi_\ell^m(\mathbf{x}_m)$ denotes the probability of the m-th mobile HAN being connected to the ℓ-th DAU conditioned to the position $\mathbf{x}_m$.[5]

Since a mobile HAN can be simultaneously under the coverage of multiple NANs, different connection choices, such as highest SNR or RSSI, and consequently different expressions for $\xi_\ell^m(\mathbf{x}_m)$, are possible. In the following, we assume for the sake of explanation that the m-th mobile HAN chooses by chance the NAN to connect with. This is reasonable when no a-priori information, as the quality of service provided by the NANs or the trajectory followed by the m-HAN, is available. It results:

$$\xi_\ell^m(\mathbf{x}_m) = \begin{cases} \dfrac{1}{|\Gamma_m(\mathbf{x}_m)|} & \text{if } \|\mathbf{x}_m - \mathbf{x}_\ell\| \le R_\ell \\ 0 & \text{otherwise} \end{cases} \qquad (5)$$

with $\Gamma_m(\mathbf{x}_m) = \{\omega_n \in \Omega : \|\mathbf{x}_m - \mathbf{x}_n\| \le R_n\}$ denoting the set of NANs covering position $\mathbf{x}_m$ of the m-th mobile HAN.

We provide an intuitive explanation of eq. (5) through the example depicted in Figure 2. Let us suppose that the m-th mobile HAN in the steady-state position x_m is under the coverage of three different NANs. In the figure, such overlapping region is indicated with the hashed black lines. Then the m-th mobile HAN is associated to each of this three NANs with a probability $\xi_\ell^m(\mathbf{x}_m)$ equal to 1/3.

The connection probability is exploited in the following to derive the overall activity probability (Theorem 1) that in turns is used in the proposed optimization problem. To this aim the preliminary result reported in Lemma 1 is needed.

Lemma 1 (Mobility-Aware Activity Probability): The mobility-aware activity probability P_ℓ^c, i.e., the probability that the ℓ-th NAN $\in \Lambda_\omega$ is using the TVWS channel c in the arbitrary time slot k by accounting for the mobility patterns of the mobile HANs is given by:

$$P_\ell^c = \sum_{k=1}^{S_\ell} q_k^c p_{h_k}^c + q_{S_\ell+1}^c \sum_{p=1}^{M} Q_{m_p, \ell}^c \psi_\ell^{m_p} p_{m_p}^c \qquad (6)$$

---

[5]Please note that in (4) there is no dependence from the time, since the probability is determined only by the steady-state spatial distribution of the considered mobile HAN.

where

$$q_k^c = \prod_{j=1}^{k-1}(1 - p_{h_j}^c) \qquad (7)$$

and

$$Q_{m_p,\ell}^c = \prod_{j=1}^{p-1}(1 - \psi_\ell^{m_j} p_{m_j}^c) \qquad (8)$$

where $p_{h_k}^c$ and $p_{m_p}^c$ denote the on-state probabilities for the h_k-th static HAN and the m_p-th mobile HAN on channel c, and ψ_ℓ^m is given in (4).

Proof: See Appendix A. ∎

Theorem 1: The overall activity probability P_O^c is given by:

$$P_O^c = 1 - \prod_{\ell \in \Lambda_\omega}(1 - P_\ell^c) \qquad (9)$$

where P_ℓ^c is derived in Lemma 1. *Proof: By noting that the overall activity probability P_O^c is the complement of the event "no NAN in Λ_ω is using the TVWS channel c" and by accounting for the result of Lemma 1, the proof follows.* ∎

B. OVERALL EXPECTED THROUGHPUT

Here, stemming from the overall activity probability P_O^c derived in Theorem 1, we evaluate in Theorem 2 the overall expected throughput achievable at the considered NAN ω by adopting the proposed strategy. To this aim, we need first to derive in Lemma 2 and in Corollary 1 two preliminary results, namely, the probability $P_a^c(\tau)$ of the TVWS channel c being sensed as available and the switching probability $P_{sw}(\tau)$.

Lemma 2 (TVWS Available Probability): Given the sensing time τ, the TVWS available probability $P_a^c(\tau)$, i.e., the probability of the TVWS channel c being declared as available by the sensing procedure is given by:

$$P_a^c(\tau) \overset{\triangle}{=} (1 - P_O^c)\left[1 - P_f^c(\epsilon, \tau)\right] + P_O^c\left[1 - P_d^c(\epsilon, \tau)\right] \qquad (10)$$

with P_O^c given in (9), and $P_d^c(\epsilon, \tau)$ and $P_f^c(\epsilon, \tau)$ given in Definitions 5 and 6, respectively.

Proof: The proof follows immediately by accounting for the proposed strategy described in Sec.III. In fact, DAU ω declares the TVWS channel c free from the neighbor NAN activities, if the sensing procedure has declared available such a channel. Since we account for real sensing, the sensing procedure can be affected by errors. Hence DAU ω can declare the TVWS channel c free even either: i) no NAN in Λ_ω is transmitting over channel c and the sensing process correctly decides (first term in (10)); ii) at least one NAN in Λ_ω is transmitting over channel c and a missing detection occurs (second term in (10)). ∎

Corollary 1 (Switching Probability): Given the sensing time τ, the switching probability $P_{sw}(\tau)$, i.e., the probability of at least one TVWS channel in $\mathcal{C} = \{c_1, \ldots, c_B\}$ being sensed by the n-th DAU as free from neighbor NAN activities, is given by:

$$P_{sw}(\tau) = 1 - \prod_{b=1}^{B}\left[P_f^{c_b}(\epsilon, \tau)(1 - P_O^{c_b}) + P_d^{c_b}(\epsilon, \tau)P_O^{c_b}\right] \qquad (11)$$

with P_O^c given in (9), and $P_d^c(\epsilon, \tau)$ and $P_f^c(\epsilon, \tau)$ resulting from Definitions 5 and 6, respectively.

Proof: By reasoning as in Theorem 1, one has:

$$P_{sw}(\tau) = 1 - \prod_{b=1}^{B}\left(1 - P_a^{c_b}(\tau)\right) \qquad (12)$$

By substituting (10) derived in Lemma 2 in (12), after some algebraic manipulations the proof follows. ∎

Remark 2 We note that the switching probability depends on: i) the traffic patterns of the closely-located NANs, through the probability $\{P_O^c\}_{c \in \mathcal{C}}$; ii) the mobility patterns of the m-HANs roaming within the network region $\mathcal{A}$, through the probability $\{P_O^c\}_{c \in \mathcal{C}}$; iii) the sensing accuracy, through the probabilities $\{P_d^c(\epsilon, \tau)\}_{c \in \mathcal{C}}$ and $\{P_f^c(\epsilon, \tau)\}_{c \in \mathcal{C}}$, which in turn depend on the selected sensing strategy and the time τ devoted to channel sensing; iv) the channel propagation conditions through the $\{P_d^c(\epsilon, \tau)\}_{c \in \mathcal{C}}$ and $\{P_f^c(\epsilon, \tau)\}_{c \in \mathcal{C}}$, since such probabilities depend on also the adopted channel models. As a consequence, the proposed analytical framework allows us to account for all the aforementioned key parameters.

Remark 3 From Corollary 1, it is evident that the switching probability satisfies the inequality (13), reported at the bottom of this page. This is reasonable: when more than one channel is free from incumbents, i.e., $B > 1$, the probability $P_{sw}(\tau)$ of using the TVWS spectrum is greater than the probability of using the TVWS spectrum when just one channel is available from incumbents.

Theorem 2: (Overall Expected Throughput): Given the sensing time τ, the overall expected throughput $\mathcal{T}^O(\tau)$ that can be achieved by adopting the proposed framework is given by:

$$\mathcal{T}^O(\tau) = \mathcal{T}^{ISM}(1 - P_{out}^{ISM})\frac{\tau}{T}$$
$$+ \left[\sum_{b=1}^{B}\prod_{u=1}^{b-1}(1 - P_a^{c_u}(\tau))\mathcal{T}_{c_b}(1 - P_{out}^{c_b})\right.$$
$$\times (1 - P_O^{c_b})(1 - P_f^{c_b}(\epsilon, \tau)) +$$
$$\left. + (1 - P_{sw}(\tau))\mathcal{T}^{ISM}(1 - P_{out}^{ISM})\right]\left(1 - \frac{\tau + \lambda}{T}\right) \qquad (14)$$

$$\min_{c_i \in \mathcal{C}}\{P_a^{c_i}(\tau)\} \leq 1 - \left(1 - \min_{c_i \in \mathcal{C}}\{P_a^{c_i}(\tau)\}\right)^B \leq P_{sw}(\tau) \leq 1 - \left(1 - \max_{c_i \in \mathcal{C}}\{P_a^{c_i}(\tau)\}\right)^B \qquad (13)$$

where $P_O^{c_i}$, $P_a^{c_i}$ and $P_{sw}(\tau)$ are derived in Theorem 1, Lemma 2 and Corollary 1, respectively. λ denotes the control packet transmission time, i.e., the time required for sharing the results about the sensing procedure within the NAN (sec. III). Finally, in (14) $\mathcal{T}_{c_i}$ and $\mathcal{T}^{ISM}$ denote the expected throughput of the TVWS channel c_i and the ISM channel, respectively, whereas $P_{out}^{c_i}$ and P_{out}^{ISM} are the outage probabilities of the TVWS channel c_i and the ISM channel as defined in Def. 7.

    Proof: See Appendix B. ∎

    Remark 4: From (14), it is clear that the overall expected throughput is function of the time devoted to the sensing procedure, either directly through the term τ/T or indirectly through the TVWS available probabilities $\{P_a^{c_i}(\tau)\}_{i=1}^{B}$ that in turn depend on the sensing accuracy through $P_f^{c_i}(\epsilon, \tau)$ and $P_d^{c_i}(\epsilon, \tau)$. As a consequence, the criterion selected to single out the value of τ affects the overall expected throughput. In the following, we discuss an optimization criterion for maximizing the overall expected throughput with respect to the sensing time.

C. CONSTRAINED THROUGHPUT MAXIMIZATION

Here, we derive in Theorem 3 the optimization criterion maximizing the overall expected throughput. To this aim, we first derive in Lemma 3 the outage probability $P_{out}(\tau)$ as a function of the sensing time τ.

First, we note that, according to the proposed switching procedure, an *overall outage event* occurs if either: i) a switching event does not happen, i.e., no TVWS channel in $\mathcal{C}$ is sensed as free from the neighbor NAN activities, and the ISM channel is in outage; ii) a switching event happens and the selected TVWS channel is in outage. Stemming from such a definition, the following Lemma is proved.

Lemma 3: (Overall Outage Probability): Given the sensing time τ, the overall outage probability $P_{out}(\tau)$ assured by the proposed analytical framework is given by:

$$P_{out}(\tau) = P_{out}^{ISM}(1 - P_{sw}(\tau))$$
$$+ \sum_{b=1}^{B} P_{out}^{c_b} P_a^{c_b}(\tau) \prod_{u=1}^{b-1}(1 - P_a^{c_u}(\tau)) \quad (15)$$

where $P_{sw}(\tau)$ is given by (12), and P_{out}^{ISM} and $\{P_{out}^{c_i}\}_{c_i \in \mathcal{C}}$ are the outage probabilities of the ISM and TVWS channels defined in Def. 7.

    Proof: The proof easily follows by accounting for the definition of overall outage event. ∎

By adopting the proposed framework, we introduce degrees of freedom that can be exploited to maximize the achievable throughput. In fact, by accounting for Def. 7 and for the result in Lemma 3, it results:

$$\min_{i \in \{1,\dots,B\}} \{P_{out}^{c_i}\} < P_{out}(\tau) < P_{out}^{ISM}, \forall \tau \in [0, T] \quad (16)$$

Hence, by jointly using the TVWS and the ISM channels, we are able to reduce the outage event rate that in turn implies an improvement of the smart grid communications reliability. Stemming from these considerations and the results

in (15) and (16), it is clear that the higher is the switching probability $P_{sw}(\tau)$, the higher is the difference between $P_{out}(\tau)$ and its upper bound, i.e., P_{out}^{ISM}. Hence, the proper tuning of the switching probability is crucial for the performance of the smart grid network.

According to the result of Corollary 1 and its subsequent remark, the switching probability $P_{sw}(\tau)$ is controlled by the parameter τ, since τ controls the sensing accuracy, i.e., $\{P_f^{c_i}(\epsilon, \tau)\}_{c_i \in \mathcal{C}}$ and $\{P_d^{c_i}(\epsilon, \tau)\}_{c_i \in \mathcal{C}}$. Hence, in order to maximize the switching probability, or equivalently, to minimize the overall outage probability, τ has to be higher as much as possible. In fact, for each considered channel, the higher is τ, the smaller is the false-alarm probability for a fixed value of the detection probability.[6] And, according to (11), $P_{sw}(\tau)$ increases as τ increases. However, as τ increases the portion of time devoted to packet transmissions decreases as well. Hence, there are two concurrent needs: 1) τ smaller as much as possible to increase the portion of time devoted to packet transmission; 2) τ higher as much as possible to minimize the overall outage probability. As a consequence, the proper setting of τ is critical for smart grid scenarios, characterized by high communication demands associated with the need of reliable communications. Stemming from these considerations, we define the optimization problem as follows:

Optimization Problem: The goal is to choose the optimal sensing time τ^* that jointly: i) maximizes the overall expected throughput $\mathcal{T}^O(\tau)$; ii) satisfies a constraint on the switching probability for a fixed value of the detection probability:

$$\tau^* = \operatorname{argmax}_{\tau \in [0,T]} \{\mathcal{T}^O(\tau)\} \quad (17)$$

Subject to :

$$P_{sw}(\tau) \geq P_{sw}^{min}$$
$$P_d^c(\epsilon, \tau) \geq P_d^*, \forall c \in \mathcal{C} \quad (18)$$

where, consistently with (13),

$$P_{sw}^{min} \leq 1 - \left(1 - \min_{c_i \in \mathcal{C}} \{P_a^{c_i}(\tau)\}\right)^B.$$

Since the n-th DAU contemporaneously senses B different channels, it is necessary to state how to fix the detection probability in (18). To this aim, the following preliminary considerations are needed.

Let us denote with $P^c(i)$ the probability that i NANs belonging to Λ_ω are using the TVWS channel $c \in \mathcal{C}$ in the arbitrary time slot k, given that channel c is occupied by the communications of at least one NAN in Λ_ω. According to Def. 5, the *coexistence detection probability $P_d^c(\epsilon, \tau)$* of

---

[6]It is well-known that it is not possible to jointly optimize the false-alarm and the detection probability [31]. Hence, a widely used criterion is to fix one of such probabilities and optimize the remaining one. In classical CR scenarios, usually, the false-alarm probability is fixed and the detection probability is maximized to protect the incumbents from harmful interference. Differently, in TVWS smart grid scenarios, it is more reasonable to fix the detection probability and to minimize the false-alarm probability, since the involved NANs are secondary networks without any priority for utilizing the spectrum.

channel c is equal to:

$$P_{\rm d}^c(\epsilon, \tau) = \sum_{i=1}^{|\Lambda_\omega|} P_{{\rm d}|i}^c(\epsilon, \tau) P^c(i) \qquad (19)$$

where $|\Lambda_\omega|$ is the cardinality of Λ_ω, $P_{{\rm d}|i}^c(\epsilon, \tau)$ denotes the coexistence detection probability conditioned by having i NANs transmitting on channel c. It is evident that, for a fixed value of τ and ϵ, the probability of declaring unavailable the sensed TVWS channel c, when channel c is indeed occupied by the communications of at least one NAN in Λ_ω, cannot be smaller than the probability of declaring unavailable the sensed TVWS channel c, when channel c is indeed occupied by the communications of just one NAN in Λ_ω, i.e.:

$$P_{\rm d}^c(\epsilon, \tau) \geq P_{{\rm d}|1}^c(\epsilon, \tau) P^c(1), \forall c \in \mathcal{C} \qquad (20)$$

where $P^c(1) = \dfrac{\sum_{\ell=1}^{|\Lambda_\omega|} P_\ell^c \prod_{\substack{k=1, \\ k \neq \ell}}^{|\Lambda_\omega|} (1 - P_k^c)}{1 - \prod_{k=1}^{|\Lambda_\omega|} (1 - P_k^c)}$, with P_ℓ^c given by (6).

(20) holds $\forall c \in \mathcal{C}$, hence also for the channel characterized by the lowest signal-to-noise ratio (SNR), say channel $\bar{c} \in \mathcal{C}$:

$$\{P_{\rm d}^c(\epsilon, \tau)\}_{\forall c \in \mathcal{C}, c \neq \bar{c}} \geq P_{\rm d}^{\bar{c}}(\epsilon, \tau) \geq P_{{\rm d}|1}^{\bar{c}}(\epsilon, \tau) P^{\bar{c}}(1) \quad (21)$$

With this in mind, and in order to deeply protect the NAN transmissions, we set the constraint on the detection probability so that the threshold ϵ is the solution of the following equality:

$$\epsilon^* : P_{{\rm d}|1}^{\bar{c}}(\epsilon^*, \tau) P^{\bar{c}}(1) = P_{\rm d}^* \qquad (22)$$

With constrained (22), we are forcing the coexistence detection probability not to be smaller than the singled out value $P_{\rm d}^*$ even in the worst detection conditions, i.e., when just one NAN in Λ_ω is active and the sensed channel is the worst. In fact, by accounting for (21), it results:

$$P_{\rm d}^c(\epsilon, \tau) \geq P_{\rm d}^*, \forall c \in \mathcal{C} \qquad (23)$$

The price of the constraint (22) is that the achievable throughput is smaller than the throughput in (17).

Specifically, by accounting for the constrain in (22), the optimization problem in (17) can be reformulated as follows:

Theorem 3: Reformulated Optimization Problem: The goal is to choose the optimal sensing time τ^* so that:

$$\tau^* = \arg \max_{\tau \in [0, T]} \{\mathcal{T}^O(\tau)\} \qquad (24)$$

*Subject to the constraint in equation (25)*

In (24), $\mathcal{T}^O(\tau)$ is derived in Theorem 2, in (25), as shown at the bottom of this page, $\gamma_{\bar{c}|1}$ is the average SNR measured on the channel $\bar{c}$ defined in (22) and (21), $\sigma_{\bar{c}}^2$ is the variance of the AWGN on channel $\bar{c}$, f_s is the sampling frequency and P_O^c is the overall activity probability on channel $c \in \mathcal{C}$ derived in (9). Finally, $\sigma_{c_w}^2$ is the highest noise variance among the ones affecting the considered TVWS channels, i.e., $\sigma_{c_w}^2 = \max_{c \in \mathcal{C}} \{\sigma_c^2\}$.

Proof: See Appendix C. ∎

V. NUMERICAL EVALUATION

In this section, we evaluate the performance of the proposed switching algorithm by adopting, as a case study, a Smart Grid based on IEEE 802.11af wireless technology for the TVWS channels and IEEE 802.11b[7] wireless technology for the ISM band.
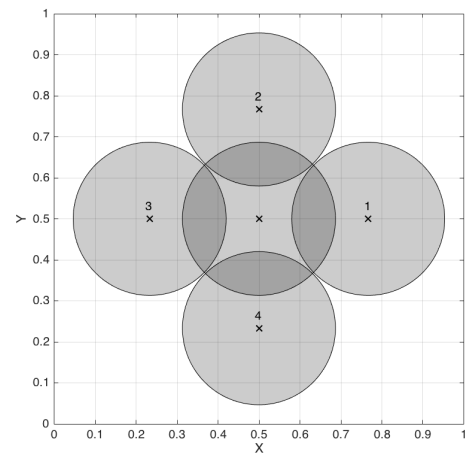
FIGURE 3. 5 closely-located NANs within the squared normalized network region $\mathcal{A}/a = [0, 1] \times [0, 1]$. The dark areas denote the overlapping regions of the DAU coverage ranges.

The considered topology is shown in Figure 3, with NAN ω, i.e., the NAN of interest, placed at the center of a squared region $\mathcal{A} = [0, a] \times [0, a]$. The mobile HANs roam within the region according to a widely adopted mobility model [32], namely, the Random Walk. The simulation set, summarized in Table 1, is as follows: up to $B = 3$ TVWS channels are available to smart grid access and, by adopting 6MHz wide channels, the data rate achievable with IEEE 802.11af is up to 26.7Mbit/s. Accordingly, by assuming a control packet size mainly depending on the physical preamble/header, we set $\lambda = 54\mu s$. Finally, the data rate achievable on the ISM band is up to 11Mbit/s.

[7]It is well known that IEEE 802.11b provides larger transmission ranges with respect to higher-throughput standard versions, such as IEEE 802.11g/n.
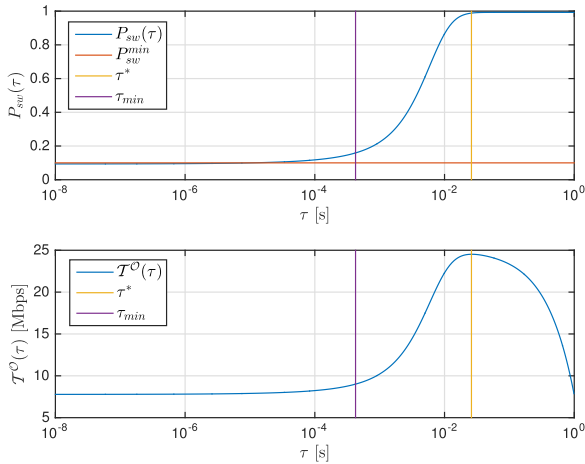
$$\tau^* \geq \tau_{\min} = \frac{\left[\sigma_{c_w}^2 Q^{-1} \left(\dfrac{\sqrt[B]{1 - P_{\rm sw}^{\min}} - \max_{c \in \mathcal{C}} \{P_O^c\}}{\max_{c \in \mathcal{C}} \{1 - P_O^c\}} \right) - Q^{-1} \left(\dfrac{P_{\rm d}^*}{P^{\bar{c}}(1)} \right) \sigma_{\bar{c}}^2 \sqrt{1 + 2\gamma_{\bar{c}|1}} \right]^2}{f_s \left[\sigma_{\bar{c}}^2 (1 + \gamma_{\bar{c}|1}) - \sigma_{c_w}^2 \right]^2} \qquad (25)$$

FIGURE 4. Throughput achievable by adopting the proposed switching procedure versus the sensing time τ.

In Figure 4, we report (lower plot) the achievable throughput (14) as a function of τ, when the mobile HANs are roaming according to the Random Walk. Specifically, we report: i) the sensing time τ^* in (24) maximizing the achievable throughput; ii) the minimum value of the sensing time τ_{min} derived in (25) jointly satisfying the switching probability and the detection probability constraints in (18) and (22), respectively; iii) the achievable throughput (14) as a function of τ. First, we note that the theoretical analysis is validated. Indeed, the value of the sensing time τ^* maximizing the achievable throughput is greater than the lower bound τ_{min} in (25). Moreover, in the same figure, we also report (higher plot) the switching probability as a function of τ. Again, the theoretical analysis is validated, since for any value of $\tau \geq \tau_{min}$, the switching probability $P_{sw}(\tau)$ satisfies the imposed constraint, i.e., $P_{sw}(\tau) \geq P_{sw}^{min}$.
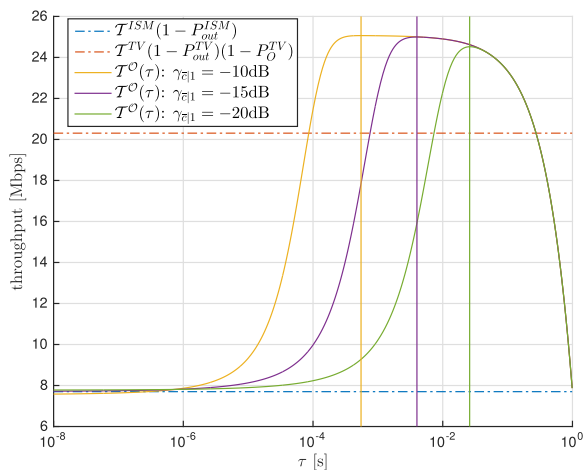

FIGURE 5. Throughput achievable by adopting the proposed switching procedure versus the sensing time τ for different values of the signal-to-noise ratio $\gamma_{\bar{c}|1}$.

In Figure 5, we report the achievable throughput (14) as a function of τ for different values of the SNR $\gamma_{\bar{c}|1}$ on the

worst channel $\bar{c}$, defined in (21). We note that the achievable throughput reaches its maximum for smaller values of τ as $\gamma_{\bar{c}|1}$ increases. This is reasonable, since the false-alarm probability decreases for a given value of τ as $\gamma_{\bar{c}|1}$ increases. Hence, the optimal value τ^* of the sensing time, derived in Theorem 3, decreases considerably as $\gamma_{\bar{c}|1}$ increases. In particular, we note that, by increasing $\gamma_{\bar{c}|1}$ from -15dB to -10dB, the sensing time decreases of roughly one order of magnitude. This in turn implies a larger time interval devoted to the data transmission. In the same figure we report two additional curves: i) the throughput $\mathcal{T}^{ISM}(1 - P_{out}^{ISM})$ achievable by using only the ISM band; ii) the throughput $\mathcal{T}^{TV}(1 - P_{out}^{TV})(1 - P_{\mathcal{O}}^{TV})$ achievable by using only the best TVWS channel. We observe that the proposed switching procedure, by setting the sensing time according to the optimization criterion given in Theorem 3, i.e., $\tau \geq \tau^*$, assures an achievable throughput always higher than all the aforementioned procedures.
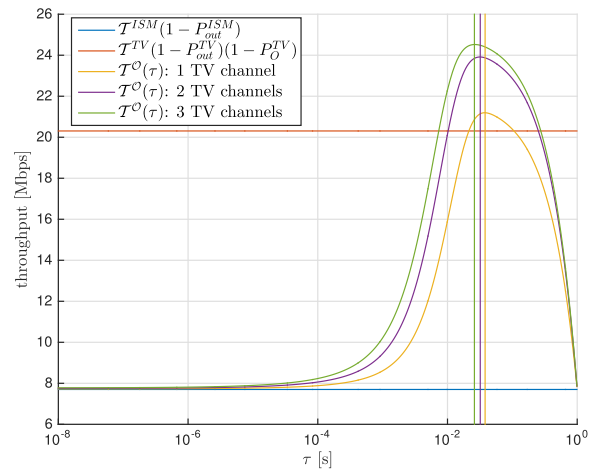

FIGURE 6. Throughput achievable by adopting the proposed switching procedure versus the sensing time τ for three different TVWS channel set.

In Figure 6 we report the achievable throughput (24) as a function of τ, when the set $\mathcal{C}$ of TVWS channels declared free from incumbents by the WSDB is constituted by one, two or three channels, respectively. As expected, the achievable throughput increases when the number of free TVWS channels increases as well. This is reasonable since the considered NAN has more opportunities to utilize the TVWS spectrum. In the same figure we also report the throughputs $\mathcal{T}^{ISM}(1 - P_{out}^{ISM})$ and $\mathcal{T}^{TV}(1 - P_{out}^{TV})(1 - P_{\mathcal{O}}^{TV})$ achievable by using only the ISM band and the best TVWS channel, respectively. We observe that the proposed switching procedure assures not only an achievable throughput always higher than all the aforementioned procedure for $\tau \geq \tau^*$, but also a smaller outage rate due to the constraint imposed on the switching probability in Theorem 3. Hence, the proposed switching procedure improves the smart grid performance in terms of reliability as well as data-rate, since it overcomes: i) the intermittent utilization of the TVWS channels due to

either the incumbent protection or the presence of interfering NANs; ii) the high outage rate of the ISM band.

Furthermore, we note that the throughput achievable with the proposed switching procedure exhibits an almost constant behavior for a wide interval of sensing time values greater than τ^*. This constitutes a very important result since it confirms that the proposed strategy improves the smart grid performance in terms of reliability.

This result is confirmed by Figure 7, where we report the throughput of the proposed switching procedure $\mathcal{T}(\tau^*)$ evaluated for the sensing time τ^* derived in Theorem 3, as function of the time. The aim of this experiment is twofold. First, we want to assess the performance of the proposed strategy in presence of realistic channel models for both the ISM and the TV bands. Furthermore, we want to show that the proposed strategy is able to account for the SG requirements in terms of reliability, latency and data rate.
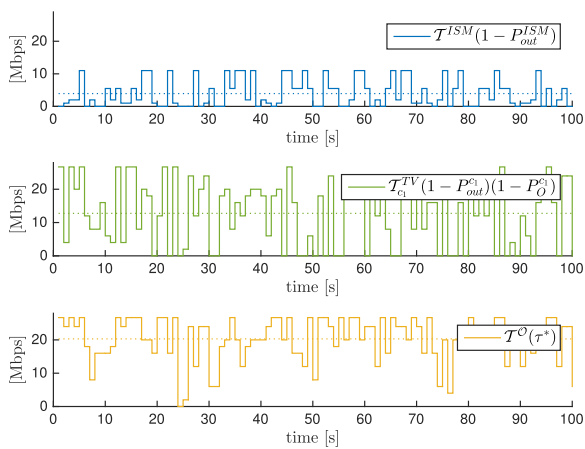
FIGURE 7. Throughput of the proposed switching procedure evaluated at the optimal sensing time τ^* versus the simulation time, compared with the intermittent throughput of the ISM band as well as the TVWS channel. Dotted lines representing the average throughput achieved in the considered time horizon.

According to the IEEE standards, the data rate achievable on the ISM band varies between 1 and 11Mbps, whereas the data rate achievable on each TVWS channel varies between 2 and 26.7 Mbps. First, we observe that the throughput achieved by the proposed strategy (lowest panel in Figure 7) is greater than the throughput achievable by exclusively using either the ISM (highest panel) or the arbitrary TV channel (central panel) in each time slot. Then we note that, by averaging on the considered time horizon, the proposed strategy achieves a mean throughput exceeding 20Mbps, with a gain roughly equal to 60% with respect to the average throughput achievable by exclusively using the TVWS spectrum and with a gain roughly equal to 510% with respect to the average throughput achievable by exclusively using the ISM spectrum.

Furthermore we observe that, at time $t = 25$ seconds, $\mathcal{T}(\tau^*)$ decreases to zero since at this time no channel (either ISM or TVWS) is available. This unavailability is evident from Figure 8, where we report both: i) the channel states for
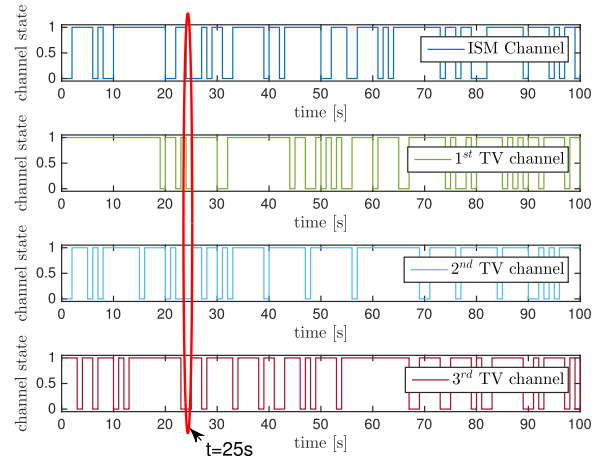
FIGURE 8. Channel state versus simulation time for ISM band and the TVWS channels.

the ISM spectrum by accounting for the outage events; ii) the channel states for the TVWS channels in $\mathcal{C}$, by accounting for both the outage and the presence of neighbor NANs activities. Clearly, as long as no TVWS channel is available, the throughput remains equal to the value assured by the ISM band. Nevertheless, we can observe that the proposed strategy guarantees a steady throughput maximization, since it is able to take full advantage from the exploitation of any available channel. Indeed, this behavior is particularly valuable in scenarios characterized by tight requirements as the SGNs.

VI. CONCLUSIONS

In this paper we studied the problem of exploiting the TV White Space spectrum for Smart Grid Networks in urban scenarios characterized by grid node mobility. Specifically, we proposed an optimal switching procedure, aiming to maximize the achievable throughput at an arbitrary Neighbor Area Network (NAN), by accounting for the presence of interfering NANs on the TVWS channels through either their traffic patterns or their mobility patterns. We proved that the proposed switching procedure is able to jointly reduce the outage event rate and increase the achievable throughput. Hence, the proposed procedure significantly improves the smart grid performance in terms of reliability, latency and data-rate. Moreover, we optimized the switching procedure by providing the closed-form expression of the sensing time that maximizes the achievable throughput under the constraint of bounding the outage rate at a given value. Finally we validated the theoretical analysis through extensive numerical simulations.

APPENDIX A
PROOF OF LEMMA 1

By accounting for Definition 3, the probability that the ℓ-th NAN $\in \Lambda_\omega$ is using the TVWS channel $c \in \mathcal{C}$ in the arbitrary time slot k, is the probability that at least one of its static HAN is using such a channel or that at least one of the mobile HANs connected to the ℓ-th DAU is using such a channel.

With this in mind, and by accounting for the addition rule of mutually exclusive events, we can write the probability of at least one static HAN using channel c as:

$$p_{h_1}^c + (1 - p_{h_1}^c)p_{h_2}^c + \ldots + \prod_{j=1}^{S_\ell - 1}(1 - p_{h_j}^c) \quad (26)$$

Hence, by adopting the same reasoning for the probability of at least one of the mobile HANs using channel c and by accounting for (7) and (8), the thesis follows

APPENDIX B
PROOF OF THEOREM 2

According to the proposed switching strategy (see Sec. III), the considered DAU is responsible for the sensing procedure. Hence in the time τ its HANs use the ISM channel. This consideration justifies the first term in (14). After that the sensing procedure is completed, the DAU instructs within the time λ, through a control packet, if and which TVWS channels among the available one $\mathcal{C} = \{c_1, \ldots, c_B\}$ can be used by its HANs. Specifically, the TVWS channel c_i is selected if the TVWS channels $\{c_b\}_{b=1}^{i-1}$ with higher priority (Section III) are sensed occupied by the DAU and either: i) with probability $P_O^{c_b}(1 - P_d^{c_i}(\epsilon, \tau))$, the TVWS channel c_i is busy but a missing-detection event occurs; ii) with probability $(1 - P_O^{c_i})(1 - P_f^{c_i}(\epsilon, \tau))$, the TVWS channel c_i is available and the sensing process correctly decides. However, only the latter event contributes to the data rate, since during the former event the packet transmission fails due to the collision with the other NANs transmissions (assuming that a capture event does not occur). If none of the TVWS channels is sensed free from the neighbor NAN transmission, the DAU instructs its NANs to use the ISM channel. Clearly, the NANs can transmit over the ISM channel only if the ISM channel is not in outage, i.e., with probability $(1 - P_{out}^{ISM})$. Hence, the thesis follows.

APPENDIX C
PROOF OF THEOREM 3

By accounting for (10), (13) can be rewritten as:

$$1 - \left[\max_{c \in \mathcal{C}} \{P_f^c(\epsilon, \tau)\} \max_{c \in \mathcal{C}} \{1 - P_O^c\} + \max_{c \in \mathcal{C}} \{P_O^c\} \right]^B$$

$$\leq 1 - \left[\max_{c \in \mathcal{C}} \{P_f^c(\epsilon, \tau)(1 - P_O^c) + P_O^c\} \right]^B$$

$$\leq 1 - \left(1 - \min_{c \in \mathcal{C}}\{P_a^c(\tau)\}\right)^B \leq P_{sw}(\tau) \quad (27)$$

Hence, the constraint $P_{sw}^{min} \leq P_{sw}(\tau)$ in (18), consistently with (13), can be set as follows:

$$P_{sw}^{min} \leq 1 - \left[\max_{c \in \mathcal{C}} \{P_f^c(\epsilon, \tau)\} \max_{c \in \mathcal{C}} \{1 - P_O^c\} + \max_{c \in \mathcal{C}} \{P_O^c\} \right]^B$$

$$\Longleftrightarrow \max_{c \in \mathcal{C}} \{P_f^c(\epsilon, \tau)\} \leq \frac{\sqrt[B]{1 - P_{sw}^{min}} - \max_{c \in \mathcal{C}} \{P_O^c\}}{\max_{c \in \mathcal{C}} \{1 - P_O^c\}} \quad (28)$$

As well-known, the channel maximizing the false-alarm probability is the one characterized by the highest noise variance, say $\sigma_{c_w}^2$, i.e., $\max_{c \in \mathcal{C}} \{P_f^c(\epsilon, \tau)\} = P_f^{c_w}(\epsilon, \tau)$.

To complete the proof, we need to express the decision threshold ϵ and the false-alarm probability, that in turn depend on the selected sensing strategy. Regarding the decision threshold, it is set to satisfy the constraint (22), i.e., $\epsilon = \epsilon^*$. Regarding the false-alarm probability, we assume to adopt the widely-used energy detector, since generally a smart grid scenario is characterized by low complexity requirement and low a-priori knowledge requirement [26]. As a consequence, by following the reasoning developed in [33], it results:

$$P_f^{c_w}(\epsilon^*, \tau) = Q\left(\frac{\epsilon^* - N\sigma_{c_w}^2}{\sqrt{N\sigma_{c_w}^4}} \right) \quad (29)$$

where $Q(\cdot)$ denotes the Q-function, $N = f_s\tau$ is the number of samples available in the sensing time τ, f_s the sampling frequency and $\sigma_{c_w}^2$ is the variance of the AWGN on channel c_w. As said, ϵ^* is the threshold satisfying the constraint (22). Hence, by expressing $P_{d|1}^{\bar{c}}(\epsilon^*, \tau)$, it results:

$$Q\left(\frac{\epsilon^* - N\sigma_{\bar{c}}^2(1 + \gamma_{\bar{c}|1})}{\sqrt{N\sigma_{\bar{c}}^4}\sqrt{1 + 2\gamma_{\bar{c}|1}}} \right) P^{\bar{c}}(1) = P_d^* \quad (30)$$

where $\sigma_{\bar{c}}^2$ is the variance of the AWGN on channel $\bar{c}$, $\gamma_{\bar{c}|1}$ is the average SNR conditioned of having only one NAN in Λ_ω transmitting on channel $\bar{c}$. By solving (30), with respect to ϵ^* one has:

$$\epsilon^* = Q^{-1}\left(\frac{P_d^*}{P^{\bar{c}}(1)} \right) \sqrt{N\sigma_{\bar{c}}^4}\sqrt{1 + 2\gamma_{\bar{c}|1}} + N\sigma_{\bar{c}}^2(1 + \gamma_{\bar{c}|1}). \quad (31)$$

By substituting (29) in (28) with ϵ^* given by (31), by accounting for the Q-function properties and by solving with respect to $N = f_s\tau$, the proof follows.

ACKNOWLEDGMENT

REFERENCES

[1] Q. Li, Z. Feng, W. Li, T. A. Gulliver, and P. Zhang, "Joint spatial and temporal spectrum sharing for demand response management in cognitive radio enabled smart grid," *IEEE Trans. Smart Grid*, vol. 5, no. 4, pp. 1993–2001, Jul. 2014.

[2] S. L. Kim, P. Kitsos, M. Nekovee, F. R. Yu, and Y. Zhang, "Guest editorial: Smart grid communications systems," *IEEE Syst. J.*, vol. 8, no. 2, pp. 417–421, Jun. 2014.

[3] R. Yu, Y. Zhang, S. Gjessing, C. Yuen, S. Xie, and M. Guizani, "Cognitive radio based hierarchical communications infrastructure for smart grid," *IEEE Netw.*, vol. 25, no. 5, pp. 6–14, Sep. 2011.

[4] A. S. Cacciapuoti, M. Caleffi, F. Marino, and L. Paura, "Enabling smart grid via TV white space cognitive radio," in *Proc. IEEE Int. Conf. Commun. (ICC) Workshop*, Jun. 2015, pp. 568–572.

[5] O. Ergul, A. O. Bicen, and O. B. Akan, "Opportunistic reliability for cognitive radio sensor actor networks in smart grid," *Ad Hoc Netw.*, vol. 41, no. 1, pp. 5–14, 2016.

[6] A. S. Cacciapuoti, M. Caleffi, and L. Paura, "On the probabilistic deployment of smart grid networks in TV white space," *Sensors*, vol. 16, no. 5, p. 671, 2016.

[7] A. A. Khan, M. H. Rehmani, and M. Reisslein, "Cognitive radio for smart grids: Survey of architectures, spectrum sensing mechanisms, and networking protocols," *IEEE Commun. Surveys Tut.*, vol. 18, no. 1, pp. 860–898, Oct. 2016.

[8] *Second Memorandum Opinion and Order in the Matter of Unlicensed Operation in the TV Broadcast Bands*, document ET docket 10-174, Federal Communications Commission (FCC), FCC, Active Regulation, Sep. 2012.

[9] *Regulatory Requirements for White Space Devices in the UHF TV Band*, Ofcom, London, U.K., Jul. 2012.

[10] "ECC Report 186: Technical and operational requirements for the operation of white spaces devices under geo-location approach."

[11] M. Caleffi and A. S. Cacciapuoti, "Database access strategy for TV white space cognitive radio networks," in *Proc. IEEE Int. Conf. Sens. Commun. Netw.*, Jul. 2014, pp. 1–5.

[12] A. S. Cacciapuoti, M. Caleffi, and L. Paura, "Optimal strategy design for enabling the coexistence of heterogeneous networks in TV white space," *IEEE Trans. Veh. Technol.*, vol. 65, no. 9, pp. 7361–7373, Sep. 2016.

[13] J. V. de Beek, J. Riihijarvi, A. Achtzehn, and P. Mahonen, "TV white space in europe," *IEEE Trans. Mobile Comput.*, vol. 11, no. 2, pp. 178–188, Feb. 2012.

[14] K. Harrison and A. Sahai, "Allowing sensing as a supplement: An approach to the weakly-localized whitespace device problem," in *Proc. IEEE Int. Symp. Dyn. Spectr. Access Netw. (DYSPAN)*, Apr. 2014, pp. 113–124.

[15] A. S. Cacciapuoti and M. Caleffi, "Interference analysis for secondary coexistence in TV white space," *IEEE Commun. Lett.*, vol. 19, no. 3, pp. 383–386, Mar. 2015.

[16] Y. J. Jang, Y. D. Ko, and S. Jeong, "Optimal design of the wireless charging electric vehicle," in *Proc. IEEE Int. Electr. Veh. Conf. (IEVC)*, Mar. 2012, pp. 1–5.

[17] S. Lee, B. Choi, and C. T. Rim, "Dynamics characterization of the inductive power transfer system for online electric vehicles by laplace phasor transform," *IEEE Trans. Power Electron.*, vol. 28, no. 12, pp. 5902–5909, Dec. 2013.

[18] Y. D. Ko and Y. J. Jang, "The optimal system design of the online electric vehicle utilizing wireless power transmission technology," *IEEE Trans. Intell. Transp. Syst.*, vol. 14, no. 3, pp. 1255–1265, Sep. 2013.

[19] M. Wang, M. Ismail, X. Shen, E. Serpedin, and K. Qaraqe, "Spatial and temporal online charging/discharging coordination for mobile PEVs," *IEEE Wireless Commun.*, vol. 22, no. 1, pp. 112–121, Feb. 2015.

[20] F. Marino, L. Paura, and R. Savoia, "On spectrum sensing optimal design in spatial-temporal domain for cognitive radio networks," *IEEE Trans. Veh. Technol.*, vol. 65, no. 10, pp. 8496–8510, Dec. 2015.

[21] A. S. Cacciapuoti, I. F. Akyildiz, and L. Paura, "Optimal primary-user mobility aware spectrum sensing design for cognitive radio networks," *IEEE J. Sel. Areas Commun.*, vol. 31, no. 11, pp. 2161–2172, Nov. 2013.

[22] R. Deng, J. Chen, X. Cao, Y. Zhang, S. Maharjan, and S. Gjessing, "Sensing-performance tradeoff in cognitive radio enabled smart grid," *IEEE Trans. Smart Grid*, vol. 4, no. 1, pp. 302–310, Mar. 2013.

[23] A. S. Cacciapuoti, M. Caleffi, F. Marino, and L. Paura, "Sensing-time optimization in cognitive radio enabling Smart Grid," in *Proc. Euro Med Telco Conf. (EMTC)*, Nov. 2014, pp. 1–6.

[24] K. M. Tan, V. K. Ramachandaramurthy, and J. Y. Yong, "Integration of electric vehicles in smart grid: A review on vehicle to grid technologies and optimization techniques," *Renew. Sustain. Energy Rev.*, vol. 53, pp. 720–732, Jan. 2016.

[25] F. Mwasilu, J. J. Justo, E.-K. Kim, T. D. Do, and J.-W. Jung, "Electric vehicles and smart grid interaction: A review on vehicle to grid and renewable energy sources integration," *Renew. Sustain. Energy Rev.*, vol. 34, pp. 501–516, Jun. 2014.

[26] R. Ma, H.-H. Chen, Y.-R. Huang, and W. Meng, "Smart grid communication: Its challenges and opportunities," *IEEE Trans. Smart Grid*, vol. 4, no. 1, pp. 36–46, Mar. 2013.

[27] *802.11af-2013: Part 11: Wireless LAN Medium Access Control (MAC) and Physical Layer (PHY) Specifications Amendment 5: Television White Spaces (TVWS) Operation*, IEEE Standard 802.11, Wireless Local Area Network Working Group, Dec. 2013.

[28] *Part 22: Cognitive Wireless RAN Medium Access Control (MAC) and Physical Layer (PHY) Specifications: Policies and Procedures for Operation in the TV Bands*, IEEE Standard 802.22, Working Group on Wireless Regional Area Networks, 2011.

[29] M. Caleffi and A. S. Cacciapuoti, "On the achievable throughput over TVWS sensor networks," *Sensors*, vol. 16, no. 4, p. 457, 2016.

[30] A. S. Cacciapuoti and M. Caleffi, "Spectrum sensing in small-scale networks: Dealing with multiple mobile PUs," *Ad Hoc Netw.*, vol. 33, pp. 209–220, Oct. 2015.

[31] I. F. Akyildiz, B. F. Lo, and R. Balakrishnan, "Cooperative spectrum sensing in cognitive radio networks: A survey," *Phys. Commun.*, vol. 4, no. 1, pp. 40–62, Mar. 2011.

[32] T. Camp, J. Boleng, and V. Davies, "A survey of mobility models for ad hoc network research," *Wireless Commun. Mobile Comput.*, vol. 2, no. 5, pp. 483–502, Sep. 2002.

[33] A. S. Cacciapuoti, M. Caleffi, D. Izzo, and L. Paura, "Cooperative spectrum sensing techniques with temporal dispersive reporting channels," *IEEE Trans. Wireless Commun.*, vol. 10, no. 10, pp. 3392–3402, Oct. 2011.

ANGELA SARA CACCIAPUOTI (M'10–SM'16) received the Laurea (integrated B.S./M.S.) (*Summa Cum Laude*) degree in telecommunications engineering and the Ph.D. degree (Hons.) in electronic and telecommunications engineering from the University of Naples Federico II, Italy, in 2005 and 2009, respectively. From September 2010 to May 2011, she was a visiting researcher at the Broadband Wireless Networking Laboratory, Georgia Institute of Technology (USA). From June 2011 to July 2011, she was a visiting researcher at the NaNoNetworking Center in Catalunya (N3Cat), Universitat Politécnica de Catalunya (Spain). In 2011 and in 2012, she joined again the Broadband Wireless Networking Laboratory as a visiting researcher. She authored over 40 refereed papers in the first tier IEEE journals and the ComSoc's flagship conferences. Her current research interests are in Internet of Things, nanonetworks, 5G mobile networks, and neuronal models. She received different awards, including the Most Cited Ad Hoc Networks Articles 2011 Award. Since 2014, she has been serving as an Editor of the *Computer Networks* (Elsevier) Journal. In 2016, she was appointed to the IEEE COMSOC Young Professional Standing Committee and she currently serves as the Award Committee Chair of the inaugural IEEE ComSoc Best YP Awards.

MARCELLO CALEFFI (M'12–SM'16) received the M.S. (*summa cum laude*) degree in computer science engineering from the University of Lecce, Lecce, Italy, in 2005, and the Ph.D. degree in electronic and telecommunications engineering from the University of Naples Federico II, Naples, Italy, in 2009. From 2010 to 2011, he was with the Broadband Wireless Networking Laboratory, Georgia Institute of Technology, Atlanta, GA, USA, as a Visiting Researcher. In 2011, he was also with the NaNoNetworking Center in Catalunya, Universitat Politècnica de Catalunya, Barcelona, Spain, as a Visiting Researcher. He is currently an Assistant Professor with the DIETI Department, University of Naples Federico II, where he teaches Telematics and Mobile Communication Systems classes and supervised and graduated over 20 among B.S. and M.S. students. He co-authored over 40 journal such as the IEEE/ACM Transactions on Networking, the IEEE Transactions on Wireless Communications, the IEEE Transactions on Communications, the IEEE Transactions on Vehicular Technology, and the IEEE Internet of Things Journal and conference such as the IEEE Globecom, the IEEE ICC, the IEEE SECON, and the ACM NANOCOM publications. His research interests are in disruption wireless technologies and unconventional computing. He serves as an Editor of *Ad Hoc Networks* (Elsevier) and the IEEE Communications Letters.

FRANCESCO MARINO was born in Naples, Italy, in 1986. He received the M.E. (*summa cum laude*) degree in telecommunications engineering and the Ph.D. degree in electronic and telecommunications engineering from the University of Naples Federico II in 2012 and 2016, respectively. He is currently with Okolab S.r.l, Italian company that offers incubators for time lapse experiments, and he is responsible for the production of technical and marketing documents (manuals, photos, installation guides, catalogue, and datasheets), provider of advice, assistance, and training pertaining to the installation, operation, and maintenance of equipment. His research activities are in the area of mobile ad hoc networks, cognitive radio, smart grid, and wireless communications.

LUIGI PAURA (M'11) received the Dr.Eng. (*summa cum laude*) degree in electronic engineering from the University of Naples Federico II, Naples, Italy, in 1974. From 1979 to 1984, he was an Assistant Professor and an Associate Professor with the Department of Biomedical, Electronic, and Telecommunications Engineering, University of Naples Federico II. Since 1994, he has been a Full Professor of Telecommunications with the Department of Mathematics, University of Lecce, Lecce, Italy, and also with the Department of Information Engineering, Second University of Naples, Naples. Since 1998, he has been with the Department of Biomedical, Electronic, and Telecommunications Engineering, University of Naples Federico II. From 1985 to 1986, and in 1991, he was a Visiting Researcher with the Signal and Image Processing Laboratory, University of California at Davis, Davis, CA, USA. His research interests are mainly in digital communication systems and cognitive radio networks.

● ● ●